

X-RAY EMISSION FROM THE TYPE IC SUPERNOVA 1994I OBSERVED WITH *CHANDRA*

STEFAN IMMLER

Astronomy Department, University of Massachusetts, Amherst, MA 01003

ANDREW S. WILSON & YUICHI TERASHIMA¹

Astronomy Department, University of Maryland, College Park, MD 20742

Draft version November 1, 2018

ABSTRACT

We present two high-resolution *Chandra* X-ray observations of supernova (SN) 1994I which show, for the first time, that the interaction of the blast wave from a Type Ic SN with its surrounding circumstellar material (CSM) can give rise to soft X-ray emission. Given a 0.3–2 keV band X-ray luminosity of $L_x \sim 1 \times 10^{37}$ ergs s⁻¹ between six and seven years after the outburst of SN 1994I, and assuming the X-ray emission arises from the shock-heated CSM, we derive a pre-SN mass-loss rate of $\dot{M} \sim 1 \times 10^{-5} M_\odot \text{ yr}^{-1}$ ($v_w/10 \text{ km s}^{-1}$). Combining the results with earlier *ROSAT* observations, we construct the X-ray lightcurve of SN 1994I. A best-fit X-ray rate of decline of $L_x \propto t^{-s}$ with index $s \sim 1$ and a CSM density profile of $\rho_{\text{CSM}} \propto r^{-1.9 \pm 0.1}$ are inferred, consistent with what is expected for a constant mass-loss rate and constant wind velocity profile for the SN progenitor ($\rho_{\text{CSM}} \propto r^{-2}$).

Subject headings: supernovae: individual (SN 1994I) — stars: mass loss — X-rays: individual (SN 1994I) — X-rays: ISM

1. INTRODUCTION

The classification scheme for SNe is based on the presence or absence of hydrogen lines in their optical spectra (Type II and Type I, respectively). While Type II/Ib SNe occur during the core collapse of a massive star, Type Ia SNe are believed to originate from the deflagration or detonation of an accreting white dwarf star in a binary system. The massive ($> 10 M_\odot$) progenitor stars for the controversial Type Ic SN subclass are thought to have lost their outer hydrogen and helium layers either through stellar winds or by mass transfer to a companion, leaving behind a stripped carbon and oxygen (C+O) star. Such a ‘naked’ C+O star will later explode when its iron core collapses (e.g. Nomoto et al. 1994). The interaction of the outgoing SN shock wave with the ambient CSM, deposited either by a pre-SN stellar wind or non-conservative mass transfer to a companion, produces hot gas with characteristic temperatures in the range $T \sim 10^7$ – 10^9 K (Chevalier & Fransson 1994). Gas heated to such high temperatures produces radiation predominantly in the X-ray range. X-ray emission from this interaction is expected for all Type Ib/c and II SNe with substantial CSM established by the massive progenitors. Over the last 20 years, searches for X-ray emitting SNe have been successful for only a relatively small number of Type II’s in the near aftermath (days to months) of the explosion (see Immler & Lewin 2002 for a review article)².

By contrast, no Type Ia or Ib/c SN has ever been firmly detected in X-rays, apart from a 3.5σ excess in an *XMM-Newton* EPIC-PN image 4'' offset from the optical position of the Ic SN 2002ap (Rodríguez-Pascual et al. 2002). Hard (2–10 keV band) X-ray emission was recorded with *BeppoSax* from the position of the unusual SN 1998bw, which might be associated with a γ -ray burst event (GRB

980425; Galama et al. 1998, Pian et al. 1998). Due to the large error box of the *BeppoSax* Wide Field Camera observation (between 3' and 8', 99% confidence limit) and the rather large probability of $\sim 60\%$ that the source is a random chance coincidence, the association of the X-ray source with SN 1998bw and GRB 980425 is still tentative (Galama et al. 1998).

Evidence for soft (0.1–2.4 keV band) X-ray emission has been reported from the Type Ic SN 1994I, based on *ROSAT* HRI observations 82 days after the outburst (Immler, Pietsch & Aschenbach 1998). However, the *ROSAT* observations, with a spatial resolution of $\sim 5''$ (FWHM on-axis), were not conclusive since SN 1994I is located close to the X-ray bright nucleus of the host galaxy M51 (distance $\sim 18''$) and is embedded in a high level of extended X-ray emission from hot gas and unresolved point-like X-ray sources in the bulge of M51.

2. X-RAY OBSERVATIONS AND ANALYSIS

We used the *Chandra* X-ray observatory to search for X-ray emission from SN 1994I in X-ray images taken between six (June 6, 2000) and seven years (June 23, 2001) after the explosion (March 31, 1994; Chandler, Phillips & Rupen 1994). Our 14.9 ks and 26.8 ks *Chandra* observations were carried out with the S3 chip of the Advanced CCD Imaging Spectrometer (ACIS-S) at the focal plane of the telescope and the nucleus of the host galaxy M51 placed at the aim-point (Terashima & Wilson 2001). The superb spatial resolution (0''.5 FWHM on-axis), together with the high sensitivity of the instrument and the long combined exposure (41.7 ks), allows us to separate point-like sources from the diffuse emission in the bulge of M51 and to carry out a sensitive search for X-ray emission from SN 1994I. The co-added and adaptively smoothed *Chandra* image of the central region of M51 is presented in Fig. 1.

¹ Institute of Space and Astronautical Science, 3-1-1 Yoshinodai, Sagami-hara, Kanagawa 229-8510, Japan

² A complete list of X-ray SNe is available at <http://xray.astro.umass.edu/sne.html>

An X-ray source is detected at the position of SN 1994I in the merged *Chandra* data with a significance of $\sim 6\sigma$ in the 0.3–2 keV band using the ‘wave detect’ algorithm implemented in the CIAO data analysis package. The position of the X-ray source (R.A., Dec.(2000) = $13^{\text{h}}29^{\text{m}}54^{\text{s}}.17, +47^{\circ}11'30''.2$) is fully consistent with the radio position of the SN ($\sim 0''.5$ offset; Rupen et al. 1994). Astrometry of the M51 nucleus shows a similarly small offset between the (2–8 keV band) X-ray and radio positions ($\sim 0''.3$). Exposure corrected source counts were extracted within a radius of 3 image pixels (90% encircled energy radius at 1 keV) and corrected for the background taken in an annulus with inner and outer radii of 3.5 and 9.5 pixels, respectively (1 pixel corresponds to $0''.49$).

A spectral model has to be assumed to convert source counts into energy fluxes. We adopted an effective (0.3–2 keV band) cooling function of $\Lambda = 3 \times 10^{-23}$ ergs $\text{cm}^3 \text{s}^{-1}$ for an optically thin Raymond-Smith thermal plasma with a temperature of 10^7 K (Raymond, Cox & Smith 1976). Although the temperature is unknown, this value is consistent with theoretical expectations (Chevalier & Fransson 1994), previous X-ray observations of other SNe and the detection of SN 1994I in the soft (0.3–2 keV) X-ray band where the peak of a 10^7 K spectrum is located. The equivalent count rate to (unabsorbed) flux conversion factors are then 4×10^{-11} (ergs $\text{cm}^{-2} \text{s}^{-1}$)/(counts s^{-1}) and 3×10^{-12} (ergs $\text{cm}^{-2} \text{s}^{-1}$)/(counts s^{-1}) for the *ROSAT* HRI and *Chandra* ACIS-S3, respectively, and a Galactic foreground column density of $N_{\text{H}} = 1.3 \times 10^{20} \text{ cm}^{-2}$ (Dickey & Lockman 1990). The uncertainty of the conversion factors for optically thin thermal spectra with temperatures in the range 10^7 – 10^9 K is $\sim 15\%$. Assuming a 0.86 keV thermal bremsstrahlung spectrum (corresponding to a temperature of 10^7 K) instead of a Raymond-Smith thermal plasma increases the conversion factor by $\sim 7\%$. The *Chandra* results for the two individual observations of SN 1994I, together with previous *ROSAT* HRI results (Immler, Pietsch & Aschenbach 1998), are summarized in Table 1.

3. DISCUSSION

We used the *Chandra* and *ROSAT* data to construct a combined X-ray lightcurve of SN 1994I, which is presented in Fig. 2. A best-fit single power-law rate of decline of $f_{\text{x}} \propto t^{-s}$ with index $s = 0.9_{-0.2}^{+0.1}$ (solid line, Fig. 2) is inferred for the measurements on days 82, 2,271 and 2,639. Assuming an initial exponential rise of the X-ray luminosity after the outburst (at time t_0) of SN 1994I and a subsequent power-law decline with index s , we also parameterized the X-ray evolution as $f_{\text{x}} \propto (t - t_0)^{-s} \times e^{-\tau}$ with $\tau \propto (t - t_0)^{-\beta}$. This model has been successfully used to describe the time dependence of the radio emission of SNe (Weiler et al. 1996). The external absorption of the emission is represented by the $e^{-\tau}$ term (‘optical depth’) and the time-dependence of the optical depth is parameterized by the exponent β . In the X-ray regime, the rise could represent either decreasing absorption by material along the line of sight to the hot gas or simply non-production of X-rays in the *ROSAT* band at early times. If we adopt this strictly heuristic description, we find $s \sim 1$ and $\beta \sim 2$ (dashed line, Fig. 2). In case the *ROSAT* detection on day 82 corresponds to a pre-maximum measurement, a steeper

index of $s \sim 1.5$ is inferred (dotted line, Fig. 2). However, given the large error range of the flux measurements, s and β are not very well constrained.

While a t^{-1} rate of decline has been observed for the Type IIb SN 1999em with *Chandra* (Pooley et al. 2002), faster rates of decline have been reported for the Ic SN 1998bw ($s = 1.4$), inferred from the tentative hard (2–10 keV) band *BeppoSax* data (Pian et al. 1999), the Ic radio SN 1990B ($s = 1.3$) and the Ib radio SNe 1983N ($s = 1.6$) and 1984L ($s = 1.5$; Van Dyk et al. 1993). By contrast, the long-term X-ray lightcurve of the IIb SN 1993J is best described by a slow rate of decline with $s = 0.27$ (Immler, Aschenbach & Wang 2001).

The X-ray emitting material could be either shocked SN ejecta (reverse shock) or shocked CSM (forward shock; Chevalier & Fransson 1994). The lack of time-dependent X-ray spectroscopy precludes a distinction but, as we shall see, the X-ray lightcurve is consistent with the latter model with a constant pre-SN mass loss rate ($\rho_{\text{CSM}} \propto r^{-2}$). Alternatively, the CSM might result from a non-conservative mass-transfer to the companion star, leading to the formation of a flattened or disk-like H and He-rich shell (Nomoto et al. 1994). In this case a CSM profile flatter than $\rho_{\text{CSM}} \propto r^{-2}$ is expected due to the non-spherically symmetric geometry of the mass-transfer.

In the stellar wind scenario the continuum equation requires a mass-loss rate of $\dot{M} = 4\pi r^2 \rho_{\text{w}}(r) \times v_{\text{w}}(r)$ through a sphere of radius r . After the SN shock plows through the CSM, its density is $\rho_{\text{CSM}} = 4\rho_{\text{w}}$ (Fransson, Lundqvist & Chevalier 1996). The X-ray luminosity of the shock-heated CSM is $L_{\text{x}} = \Lambda(T)dVn^2$, where dV is the volume, $n = \rho_{\text{CSM}}/m$ is the number density of the shocked CSM and m is the mean mass per particle (2.1×10^{-27} kg for a H+He plasma). We thus obtain $L_{\text{x}} = 4/(\pi m^2)\Lambda(T) \times (\dot{M}/v_{\text{w}})^2 \times (v_{\text{s}}t)^{-1}$. The observed X-ray rate of decline (t^{-1}) is consistent with this description if $\Lambda(T)$, \dot{M}/v_{w} and v_{s} are constant. We can hence use the observed X-ray luminosity at time t after the outburst to measure the ratio \dot{M}/v_{w} assuming a constant shell expansion velocity v_{s} . Given our observed X-ray luminosities (Table 1) and assuming a shell expansion velocity of $v_{\text{s}} = 16,500 \text{ km s}^{-1}$ (Filippenko et al. 1995) we derive a mass-loss rate of $\dot{M} \sim 1 \times 10^{-5} M_{\odot} \text{ yr}^{-1}$ ($v_{\text{w}}/10 \text{ km s}^{-1}$) consistent with all three detections and the *ROSAT* upper limit on day 1,368.

It should be noted, however, that a single power-law model can only be reconciled with the data obtained on days 82–2,639, but not with the early *ROSAT* upper limit on day 52 (see Fig. 2). This is indicative that the above model might be incomplete for early epochs. The addition of an exponential term describing the rise during the early phase of the emission leads to a fit that is in agreement with all measurements in case the *ROSAT* detection on day 82 was a post-maximum measurement ($s \sim 1$). By contrast, the model with a steeper rate of decline ($s \sim 1.5$), which postulates that the early *ROSAT* detection corresponds to a pre-maximum measurement, is in conflict with a $\rho_{\text{CSM}} \propto r^{-2}$ profile.

Table 1 summarizes the CSM number density n for the different radii $r = v_{\text{s}} \times t$ corresponding to the dates of the observations. As was already claimed based on the early *ROSAT* data (Immler, Pietsch & Aschenbach 1998), the

3σ upper limit for the CSM density at $r = 2.0 \times 10^{17}$ cm (day 1,368) is lower than that at 1.2×10^{16} cm (day 82). Our *Chandra* results at 3.2 and 3.8×10^{17} cm (days 2,271 and 2,639, respectively) clearly support these early indications for a decreasing CSM density profile (see Table 1). The combined *ROSAT* and *Chandra* data of SN 1994I give a best-fit profile of $\rho_{\text{CSM}} \propto r^{-1.9 \pm 0.1}$.

The only SN for which a CSM density profile has been constructed from X-ray measurements is SN 1993J (Type IIb with a progenitor of $\sim 15M_{\odot}$), based on long-term monitoring with *ROSAT* between six days and five years after the outburst (Immler, Aschenbach & Wang 2001). A comparison between the CSM profiles of the two SNe is presented in Fig. 3. Although the CSM density profile of SN 1993J is significantly flatter ($\rho_{\text{CSM}} \propto r^{-1.6}$) than that of SN 1994I, the two SNe have a similar CSM number density of $\sim 10^{6.5} \text{ cm}^{-3}$ at a radius of $r \sim 5 \times 10^{15}$ cm from

the site of the explosion (cf. Fig. 3).

Given that both the X-ray rate of decline ($L_x \propto t^{-1}$) and the CSM profile ($\rho_{\text{CSM}} \propto r^{-1.9 \pm 0.1}$) of SN 1994I are not in conflict with what is expected for a constant stellar wind speed and a constant mass-loss rate of the progenitor ($L_x \propto t^{-1}$, $\rho_{\text{CSM}} \propto r^{-2}$), it is likely that the stellar wind of the massive progenitor dominates the CSM.

We thank Roger Chevalier for helpful discussion and the referee (Bernd Aschenbach) for his comments that led to significant improvement of the manuscript. This research was supported by NASA grants NAG 5-8999 to the University of Massachusetts and NAG 81755 to the University of Maryland. Y.T. is supported by the Japan Society for the Promotion of Science Postdoctoral Fellowship for Young Scientists.

REFERENCES

- Chandler, C.J., Phillips, J. A., & Rupen, M. P. 1994, IAU Circ., No. 5978
 Chevalier, R.A., & Fransson, C. 1994, ApJ, 420, 268
 Dickey, J.M., & Lockman, F.J. 1990, ARA&A, 28, 215
 Feldmeier, J.J., Ciardullo, R., & Jacoby, G.H. 1997, ApJ, 479, 231
 Filippenko, A.V., et al. 1995, ApJ, 450, L11
 Fransson, C., Lundqvist, P., & Chevalier, R.A. 1996, ApJ, 461, 993
 Galama, T.J., et al. 1998, Nature, 395, 670
 Immler, S., Pietsch, W., & Aschenbach, B. 1998, A&A, 336, L1
 Immler, S., Aschenbach, B., & Wang, Q.D. 2001, ApJ, 561, L107
 Immler, S., & Lewin, H.G. 2002, in Supernovae and Gamma-Ray Bursts, ed. K. W. Weiler (Springer Publisher), astro-ph/0202231
 Nomoto, K., et al. 1994, Nature, 371, 227
 Pian, E., et al. 1999, A&AS, 138, 463
 Pooley, D., et al. 2002, ApJ in press, astro-ph/0103196
 Raymond, J.C., Cox, D.P., & Smith, B.W. 1976, ApJ, 204, 290
 Rodriguez-Pascual, P.M., et al. 2002, IAU Circ., No. 7821
 Rupen, M.P., et al. 1994, IAU Circ., No. 5963
 Terashima, Y., & Wilson, A. S. 2001, ApJ, 560, 139
 Van Dyk, S., Sramek, R.A., Weiler, K.W., & Panagia, N. 1993, ApJ, 419, 162
 Weiler, K.W., et al. 1986, ApJ, 301, 790

TABLE 1
X-RAY PROPERTIES OF SN 1994I

| Day ^(a) | Instrument | Count Rate (10^{-4} cts s^{-1}) | f_x ^(b) (10^{-15}) | L_x ^(c) (10^{37}) | \dot{M} ^(d) (10^{-5}) | $\log n$ ^(e) (cm^{-3}) |
|--------------------|-----------------------|---|--|---------------------------------------|---|---|
| 52 | <i>ROSAT</i> HRI | < 3.1 | < 12.9 | < 10.9 | < 0.5 | < 5.9 |
| 82 | <i>ROSAT</i> HRI | 5.2 ± 1.7 | 21.6 ± 5.0 | 18.2 ± 4.2 | 0.7 ± 0.4 | 5.7 |
| 1,368 | <i>ROSAT</i> HRI | < 8.4 | < 34.8 | < 29.4 | < 3.8 | < 4.0 |
| 2,271 | <i>Chandra</i> ACIS-S | 5.5 ± 2.2 | 1.7 ± 0.7 | 1.4 ± 0.5 | 1.1 ± 0.7 | 3.0 |
| 2,639 | <i>Chandra</i> ACIS-S | 4.6 ± 1.6 | 1.4 ± 0.5 | 1.2 ± 0.4 | 1.1 ± 0.7 | 2.9 |

^(a) day after the outburst of SN 1994I (March 31, 1994; Chandler, Phillips & Rupen 1994)

^(b) 0.3–2 keV band flux in units of 10^{-15} ergs cm^{-2} s^{-1} for a 10^7 K thermal plasma spectrum and a Galactic foreground column density of $N_{\text{H}} = 1.3 \times 10^{20}$ cm^{-2} (Dickey & Lockman 1990)

^(c) 0.3–2 keV band luminosity in units of 10^{37} ergs s^{-1} for an assumed distance of $d = 8.4$ Mpc (Feldmeier, Ciardullo & Jacoby 1997)

^(d) pre-SN mass-loss rate in units of $10^{-5} M_{\odot} \text{ yr}^{-1}$

^(e) post-shock CSM number density

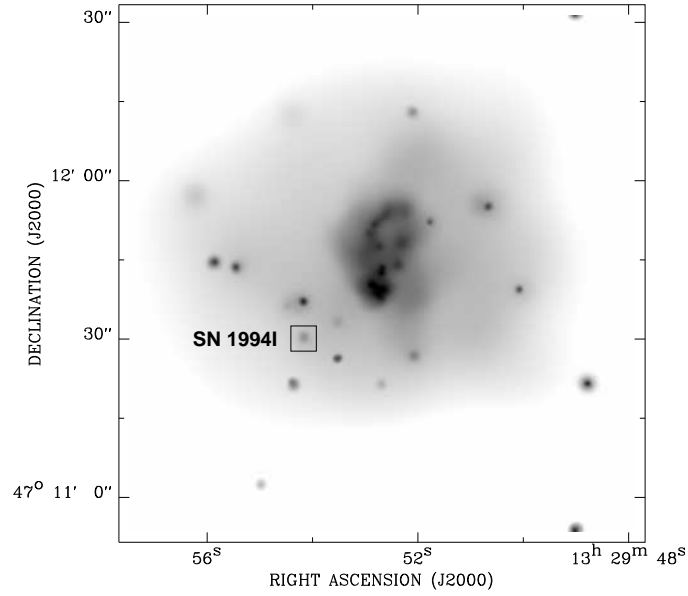


FIG. 1.— *Chandra* ACIS-S soft (0.3–2 keV) band X-ray image of the central region of M51. The image was adaptively smoothed to achieve a signal-to-noise ratio in the range 3–5 and is plotted in logarithmic greyscale. The position of SN 1994I is marked by a box and the nucleus of M51 is at the center of the image.

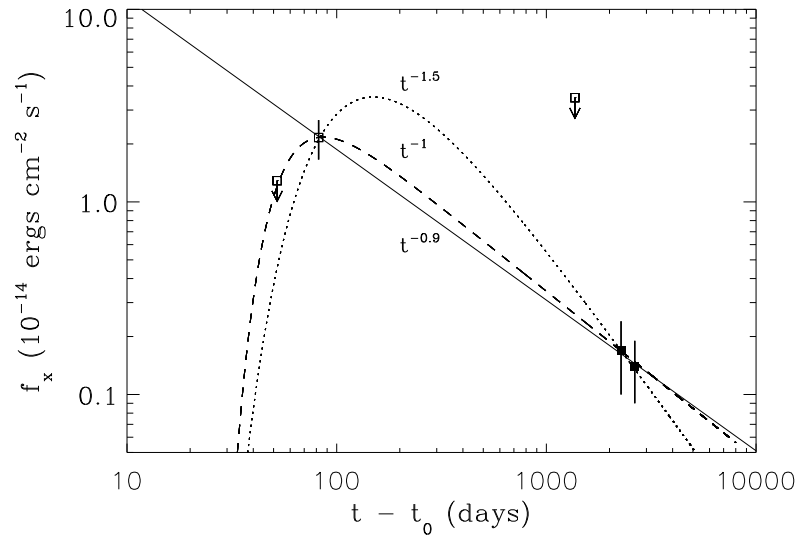


FIG. 2.— Soft (0.3–2 keV) band X-ray lightcurve of SN 1994I. The *Chandra* detections are marked by filled boxes, open boxes indicate the early *ROSAT* HRI detection and 3σ upper limits. Error bars are $\pm 1\sigma$ statistical errors. Time is given in days after the outburst. The solid line represents a power-law fit to the detections at days 82, 2,271 and 2,639. The dashed and dotted lines represent models including an $e^{-\tau}$ term (see Section 3).

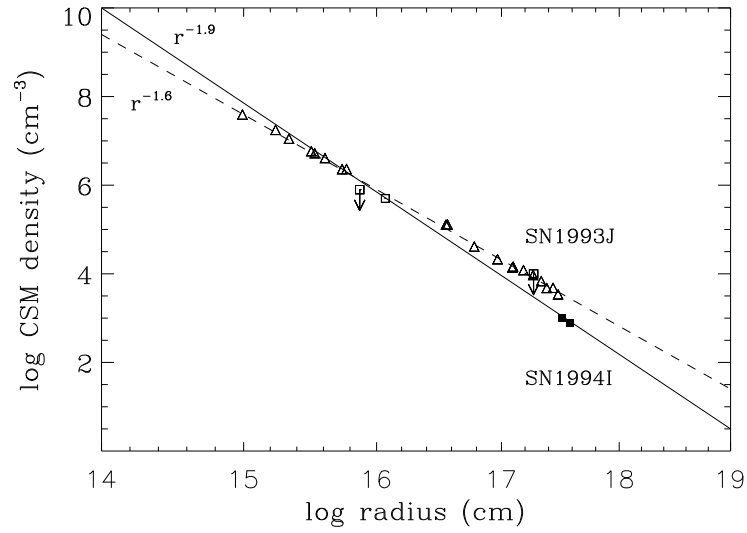


FIG. 3.— Circumstellar matter density profile as a function of SN shell expansion radius. The solid line gives the best-fit CSM density profile of $\rho_{\text{CSM}} \propto r^{-1.9}$ for the *ROSAT* (open boxes) and *Chandra* (filled boxes) measurements of SN 1994I. The CSM density profile with $\rho_{\text{CSM}} \propto r^{-1.6}$ based on *ROSAT* observations of SN 1993J is drawn for comparison (dashed line and open triangles; Immler, Aschenbach & Wang 2001).